IOPscience iopscience.iop.org

Home Search Collections Journals About Contact us My IOPscience

Analytical formula of the transmission probabilities across arbitrary potential barriers

This article has been downloaded from IOPscience. Please scroll down to see the full text article.

2005 J. Phys. A: Math. Gen. 38 5771

(http://iopscience.iop.org/0305-4470/38/25/012)

View the table of contents for this issue, or go to the journal homepage for more

Download details:
IP Address: 171.66.16.92
The article was downloaded on 03/06/2010 at 03:49

Please note that terms and conditions apply.

Institute of Physics Publishing Journal of Physics A: Mathematical and General

J. Phys. A: Math. Gen. **38** (2005) 5771–5780 doi:10.1088/0305-4470/38/25/012

# Analytical formula of the transmission probabilities across arbitrary potential barriers

**Ying He, Zhuangqi Cao and Qishun Shen**

Institute of Optics and Photonics, Shanghai Jiao Tong University, Shanghai 200240, People's Republic of China

E-mail: yinghe@sjtu.edu.cn

Received 23 October 2004, in final form 21 April 2005
Published 8 June 2005
Online at stacks.iop.org/JPhysA/38/5771

**Abstract**

The analytical transfer matrix method is applied to the evaluation of the tunnelling in the semiconductor heterostructures. An analytical formula of the transmission probabilities across arbitrary shaped potential barriers which includes the variations of the effective masses has been developed in this paper. Various potential barrier structures are analysed and the results are of high precision. Tunnelling resonance is obtained for the double-barrier structure. We can correlate the energy location of the peaks of the transmission probability with the bound state energies of the included potential wells through our analytical transfer matrix method.

PACS numbers: 73.40.Gk, 73.40.Lq, 85.30.De

## 1. Introduction

With recent advances in semiconductor growth techniques, it has become possible to fabricate multiple barriers and periodic potential structures of good quality. Fabrication of these structures results in a considerable increase in research activity towards the development of novel optoelectronic devices [1, 2]. To understand the physics properties of these heterostructure devices, one has to get the tunnelling properties for different systems. Recently, resonant tunnelling through single-barrier heterostructures, double-barrier structures and multibarrier systems has been widely investigated [3–7]. A knowledge of the tunnelling coefficient is an important factor, for example, to determine the *I–V* characters of these devices. Tunnelling provides insight into many interesting processes such as lasing in quantum-well laser structures and electron transport in planar doped barrier devices. Investigation of the transmission probabilities helps to develop the heterostructure devices inversely.

Several methods have been reported in the calculation of the transmission probability across the potential barriers [8, 9]. The conventional method of determining the transmission probability is the WKB approximation method. However, it does not take into account

 © 2005 IOP Publishing Ltd Printed in the UK 

the detailed structure of a given potential below the incident electron energy, and it fails to predict the fine structures of the transmission probability. Airy's function-based computations result in numerical overflow which significantly reduces the computational efficiency of the method at low-applied biases [10, 11]. Many other methods dealing with these problems are cumbersome to implement, such as Monte Carlo method and the finite element method. Some other methods have been developed in the calculation of the transmission probability in recent years. For an example, equivalent transmission-line model is used to analyse resonant tunnelling in multilayered heterostructures [12], and the transfer matrix method in terms of Airy's functions is improved to eliminate the numerical problems which arise in the computation of the transmission coefficient [13]. In this paper we use the analytical transfer matrix method to determine the tunnelling coefficients for any shaped potential barriers explicitly. Our method is not a matrix manipulation involving straightforward multiplication of matrices, as general transfer matrix methods do [14]. We present an exact analytical formula on the basis of the transfer matrix method. Furthermore, the variation of the effective mass is directly included into the analytical formula, by which we can explore the tunnelling probabilities for any structure made of arbitrary semiconductor materials. The analytical transfer matrix method is easy to implement and gives results of high accuracy, which is more than sufficient for most applications.

## 2. Theory

In the effective-mass approximation, the time-independent Schrödinger equation in one dimension is given by

$$\left[-\frac{\mathrm{d}}{\mathrm{d}x}\frac{\hbar^2}{2m(x)}\frac{\mathrm{d}}{\mathrm{d}x}+V(x)\right]\psi(x)=E\psi(x), \tag{1}$$

where the variation in space of the particle's effective mass is expressed by $m(x)$, and $\hbar = h/2\pi$, $h$ being Planck's constant. $V(x)$ represents the potential energy variation. $E$ and $\psi(x)$ represent the energy and wavefunction. For a potential barrier with the mass dependent on the position, the transmission probability may be determined by solving the time-independent Schrödinger equation.

Consider a potential barrier with an arbitrary potential $V(x)$ in the region $x_b \leqslant x \leqslant x_f$ and with constant potential in the regions $x < x_b$ and $x > x_f$. The dependence of the mass on the position is $m(x)$. In the present calculation, we first divide the potential barrier and the position-dependent mass into segments; in every segment the potential energy $V(x_i)$ and the effective mass $m(x_i)$ can be regarded as constants. In the limit, as the divisions become finer and finer, continuous variations of the potential barrier and the effective mass will be recovered. Assuming that $x_c$ and $x_d$ are classical turning points, $x_b$ and $x_f$ are the truncation points far away from the turning points. To apply the analytical transfer matrix method, we divide the regions $(x_b, x_c)$, $(x_c, x_d)$ and $(x_d, x_f)$ into $l$, $p$ and $q$ layers with the width $d$. The transfer matrix corresponding to the $i$th segment can be written as [15]

$$M_i=\begin{bmatrix}\cos(k_i d) & -\frac{m_i}{k_i}\sin(k_i d)\\ \frac{k_i}{m_i}\sin(k_i d) & \cos(k_i d)\end{bmatrix},\qquad i=1,2,\ldots,l+p+q, \tag{2}$$

where $k_i = \sqrt{2m_i(E-V_i)}/\hbar$. $k_i$ and $V_i$ represent the wave number and the potential energy at the $i$th segment, $m_i$ is the effective mass of the particle in the $i$th region. $E$ is the energy of the incident particle.

In problems where the carrier mass changes abruptly during tunnelling, e.g., in tunnelling from InGaAs through InAlAs etc, the continuity of $\psi(x)$ and $\psi'(x)/m(x)$ has to be considered at the heterointerfaces. Applying the boundary condition, we get the matrix equation

$$\begin{bmatrix} \psi(x_b) \\ \frac{1}{m_b}\psi'(x_b) \end{bmatrix} = \prod_{i=1}^{l+p+q} M_i \begin{bmatrix} \psi(x_f) \\ \frac{1}{m_f}\psi'(x_f) \end{bmatrix}, \tag{3}$$

where $\psi(x_b)$ and $\psi(x_f)$ are the wavefunctions at the left truncation point and that at the right one, respectively. $m_b$ and $m_f$ are the effective masses at the truncation points.

We assume that a plane wave is incident from the left, and the wavefunction for $x < x_b$ and $x > x_f$ can be written as

$$\psi(x) = \begin{cases} A_0 \exp[\mathrm{i}k_b(x - x_b)] + B_0 \exp[-\mathrm{i}k_b(x - x_b)], & x < x_b \\ C_0 \exp[\mathrm{i}k_f(x - x_f)], & x > x_f, \end{cases} \tag{4}$$

where $k_b = \sqrt{2m_b(E - V(x_b))}/\hbar, k_f = \sqrt{2m_f(E - V(x_f))}/\hbar$, and $A_0, B_0, C_0$ are the amplitude coefficients to be determined.

On applying the boundary conditions that the wavefunction and its first derivative divided by the effective mass are continuous at the boundary between the two neighbouring layers, we obtain

$$\begin{bmatrix} \psi(x_i) \\ \frac{1}{m_i}\psi'(x_i) \end{bmatrix} = M_{i+1} \begin{bmatrix} \psi(x_{i+1}) \\ \frac{1}{m_{i+1}}\psi'(x_{i+1}) \end{bmatrix}, \qquad i = 0, 1, \ldots, l + p + q - 1, \tag{5}$$

where $x_i = x_b + id(i = 0, 1, 2, \ldots, l + p + q)$, and the prime denotes differentiation with respect to $x$. Both sides of equation (5) are simultaneously multiplied by the matrix $[-\psi'(x_i)/m_i, \psi(x_i)]$, then divided by $\psi(x_i)\psi(x_{i+1})$; hence equation (5) is changed into the form

$$\left[-\frac{1}{m_i}\frac{\psi'(x_i)}{\psi(x_i)}, 1\right] M_{i+1} \begin{bmatrix} 1 \\ \frac{1}{m_{i+1}}\frac{\psi'(x_{i+1})}{\psi(x_{i+1})} \end{bmatrix} = 0. \tag{6}$$

Defining

$$Q_i = -\frac{\psi'(x_i)}{\psi(x_i)}, \tag{7}$$

we get

$$\frac{Q_{i+1}}{k_{i+1}} = \tan\left[\arctan\left(\frac{m_{i+1}}{m_i}\frac{Q_i}{k_{i+1}}\right) + k_{i+1}d\right], \qquad i = 0, 1, \ldots, l + p + q - 1. \tag{8}$$

Equation (8) can be written as

$$k_{i+1}d = n\pi - \arctan\left[\frac{m_{i+1}}{m_i}\frac{Q_i}{k_{i+1}}\right] + \arctan\left[\frac{Q_{i+1}}{k_{i+1}}\right], \quad i = 0, 1, \ldots, l + p + q - 1; \quad n = 0, 1, 2\ldots \tag{9}$$

where $Q_i$ are subject to the boundary condition, $Q_0 = Q_b = -\psi'(x_b)/\psi(x_b)$.

Summing the indices $i$ from 0 to $l - 1$, we have

$$\sum_{i=0}^{l-1} k_{i+1}d + \zeta = n\pi + \arctan\left(\frac{Q_l}{k_l}\right) - \arctan\left[\frac{m_1 Q_0}{m_0 k_1}\right], \qquad n = 0, 1, 2, \ldots, \tag{10}$$

where

$$\zeta = \sum_{i=1}^{l-1}\left[\arctan\left(\frac{m_{i+1}}{m_i}\frac{Q_i}{k_{i+1}}\right) - \arctan\left(\frac{Q_i}{k_i}\right)\right]. \tag{11}$$

Considering the derivative of arctan $(m_{i+1}Q_i/m_ik_{i+1})$, we get

$$\arctan\left(\frac{m_{i+1}}{m_i}\frac{Q_i}{k_{i+1}}\right) - \arctan\left(\frac{m_i}{m_i}\frac{Q_i}{k_i}\right) = \frac{Q_i}{m_i}\frac{k_i\Delta m_i - m_i\Delta k_i}{k_i^2 + Q_i^2}. \tag{12}$$

Substituting $Q_i$ into the Schrödinger equation (1), we obtain

$$Q' = (Q^2 + k^2) + Q\frac{m'}{m}, \tag{13}$$

where $Q' = \mathrm{d}Q/\mathrm{d}x$ and $m' = \mathrm{d}m/\mathrm{d}x$.

As the width of every segment layer tends to zero, equation (11) can be written in the integral form by using equations (12) and (13):

$$\zeta = \lim_{d\to 0}\sum_{i=1}^{l-1}\left[\arctan\left(\frac{m_{i+1}}{m_i}\frac{Q_i}{k_{i+1}}\right) - \arctan\left(\frac{m_i}{m_i}\frac{Q_i}{k_i}\right)\right]$$
$$= \int_{x_b}^{x_c}\left(Q\frac{km' - mk'}{mQ' - Qm'}\right)\mathrm{d}x. \tag{14}$$

The first term in equation (10) can be integrated as $\int_{x_b}^{x_c} k\,\mathrm{d}x$. It is clear that as $d \to 0$, we have

$$k_l = \sqrt{2m_l[E - V(x_l)]}/\hbar \to \sqrt{2m_l[E - V(x_c)]}/\hbar = 0. \tag{15}$$

Meanwhile, $Q_l$ is positive, so $\arctan(Q_l/k_l) = \pi/2$. This indicates that the half-phase loss at the left turning point $x_c$ is $\pi/2$, where the electron moves from the potential well to the potential barrier.

Equation (10) can then be written as

$$\int_{x_b}^{x_c}\left(k + Q\frac{km' - mk'}{mQ' - Qm'}\right)\mathrm{d}x = \left(n + \frac{1}{2}\right)\pi - \tan^{-1}\left[\frac{m_1}{m_0}\frac{Q_0}{k_1}\right], \qquad n = 0, 1, 2, \ldots. \tag{16}$$

$Q_0$ in equation (16) is related to the coefficients $A_0$ and $B_0$, and it can be obtained from equations (4) and (7),

$$Q_0 = \mathrm{i}k_b\frac{B_0 - A_0}{B_0 + A_0}. \tag{17}$$

The reflection and transmission coefficients $R$ and $T$, defined as

$$R = |B_0|^2/|A_0|^2 \tag{18}$$

and

$$T = k_f|C_0|^2/k_b|A_0|^2, \tag{19}$$

are related by

$$R + T = 1. \tag{20}$$

The transmission coefficients, defined as the ratio of the power transmitted across the potential barriers to the power in the incident energy, can be obtained from equations (17)–(20),

$$T = 1 - R = 1 - \left|\frac{\mathrm{i}k_b + Q_0}{\mathrm{i}k_b - Q_0}\right|^2, \tag{21}$$

where the value of $Q_0$ can be derived from the analytical formula (16).

For a given potential barrier $V(x)$ and position-dependent effective mass $m(x)$, the accurate transmission probability can be obtained via our formula (16). Equation (16) is our main result.

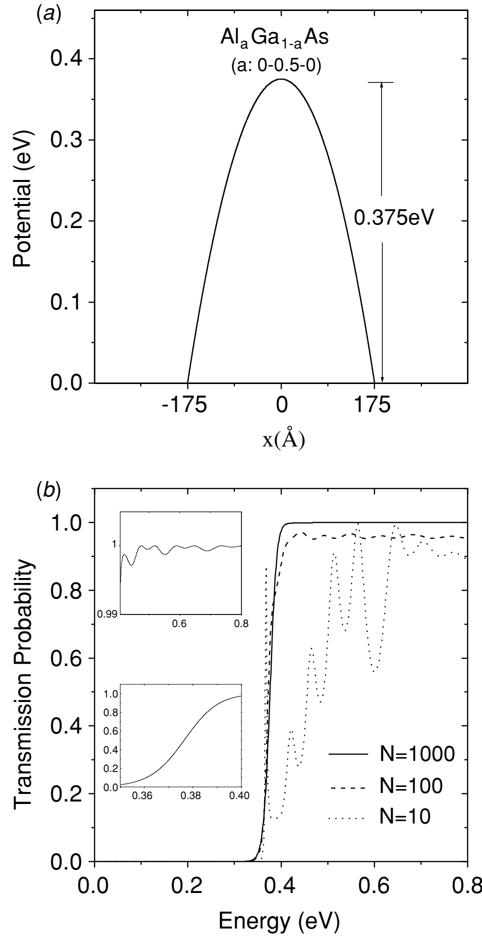


**Figure 1.** (*a*) Parabolic barrier made of $Al_aGa_{1-a}As$. (*b*) Transmission probability as a function of the incident electron energy for the structure in (*a*).

## 3. Application to heterostructures

In this section we apply the formula of transmission probability from the analytical transfer matrix method to potential barriers fabricated with semiconductor heterostructures. Various potential barrier structures will be analysed to show the capability of our method.

The single-barrier structure is first analysed. The parabolic barrier fabricated with $GaAs/Al_aGa_{1-a}As$ is shown in figure 1(*a*). The conduction-band offset was taken to be 60% of GaAs and $Al_aGa_{1-a}As$ Γ band-gap difference [16]. The parabolic barrier is 350 Å thick. For the GaAs–$Al_aGa_{1-a}As$ ($a$ : 0–0.5–0) system, assuming the variation of the composition $a$ is linear with the position $x$, we get

$$a(x) = \begin{cases} 0.5(x/175) + 0.5 & (-175 \leqslant x \leqslant 0) \\ -0.5(x/175) + 0.5 & (0 < x \leqslant 175). \end{cases} \tag{22}$$

The effective mass $m(a)$ for the system is dependent on the structure of the heterostructure, which satisfies the following equation:

$$m(a) = (0.067 + 0.083a)m_0, \tag{23}$$

where $m_0$ is the free-electron mass. The composition $a$ for GaAs is 0, so its effective mass is $0.067m_0$; while that for AlAs is 1, so the effective mass is $0.15m_0$.

Then the position-dependent effective mass can be described by

$$m(x) = \begin{cases} (0.083 \times 0.5 \times (x/175) + 0.083 \times 0.5 + 0.067)m_0 & (-175 < x \leqslant 0) \\ (-0.083 \times 0.5 \times (x/175) + 0.083 \times 0.5 + 0.067)m_0 & (0 < x < 175) \\ 0.067m_0 & (x \leqslant -175, x \geqslant 175). \end{cases} \tag{24}$$

The maximum potential energy is 0.375 eV for the parabolic barrier, as shown in figure 1($a$). The potential energy as a function of the position $x$ is as follows for the parabolic barrier:

$$V(x) = \begin{cases} -0.375(x/175)^2 + 0.375 & (-175 < x < 175) \\ 0 & (x \leqslant -175, x \geqslant 175). \end{cases} \tag{25}$$

The unit of the position $x$ is Å

From our formula (16) for arbitrary shaped barrier, the transmission probability as a function of the energy of the incident electron is obtained, which is shown in figure 1($b$). In our calculation we divide the parabolic barrier and the effective mass into 10, 100, 1000 segments respectively. The solid curve represents the transmission probability when the potential barrier and the effective mass are divided into 1000 segments. The solid curve increases from 0 to 1 rapidly, then remains flat for incident energy greater than 0.406. We have magnified the flat curve and shown it in a semilog plot in the inset. We find the solid curve oscillates around 1 slightly for incident energy greater than 0.406. This is due to the quantum mechanical tunnelling. We have also magnified the region where the incident electron energy is close to 0.375 eV in the inset of figure 1($b$), which is the potential energy at the top of the barrier. It is shown that the transmission probability increases with the increasing incident electron energy, however, the transmission probability does not reach unity at the top of the barrier. This is due to quantum mechanical reflection above the potential barrier. When we divide the barrier and the effective mass into 10 segments, the obvious oscillatory behaviour in the transmission probability is found. When we divide them into 100 segments, the oscillatory behaviour in the transmission probability weakens. The electron wavelength at the resonant states is 50 Å or so when the voltage drop value in the barrier is about 2.2 V. When the number of the section layers approaches infinity, the layer width is much smaller than the electron wavelength at the resonant states, and the calculated transmission probability tends to the accurate value. Application of our formula to the single-barrier structure produces good results.

There has been revived interest recently in the theoretical analysis of multibarrier tunnelling structures. These structures have been attracting much attention in recent years because of their electronic and optoelectronic properties. GaAs/AlAs double-barrier structures exhibit a number of interesting features, including negative differential resistance, fast response times and bistability in current–voltage response. We propose to calculate the transmission probabilities for various double-barrier structures. The double-barrier structure with a rectangular well made of GaAs and AlAs is shown in figure 2($a$). The maximum potential energy is 0.956 eV for the double-barrier structure. Position dependence of the effective mass of the electron in the various barrier and well regions is considered. The effective masses used are: $0.067m_0$ for GaAs, $0.15m_0$ for AlAs, where $m_0$ is the free-electron mass. The transmission probability for the double-barrier structure exhibits many resonance peaks, as shown in figure 2($b$). These results are in good agreement with those reported for the same structures [8, 9].

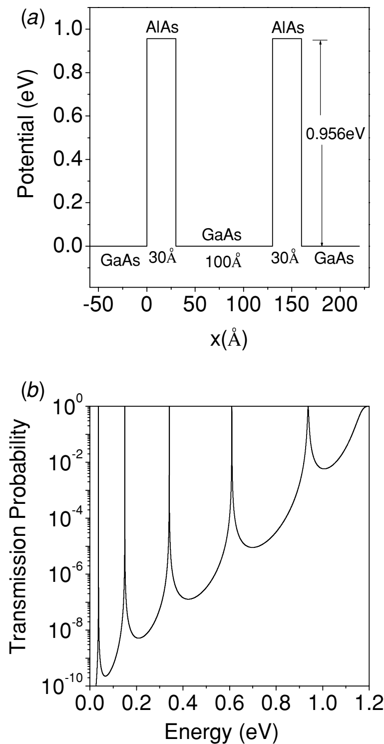


**Figure 2.** (*a*) Double barrier with a rectangular well made of GaAs and AlAs. (*b*) Transmission probability as a function of the incident electron energy for the structure in (*a*).

Applications of our formalism to the above two tunnelling structures have fully proven the validity of our method. The analytical transfer matrix formula (16) is exact in the tunnelling through the barriers. As a third example, we apply it to another double-barrier structure placed in an external electric field. It is to show intuitively the difference in the transmission probabilities when the effective masses in different regions are included or not. This structure consists of one 10 Å thick layer of a semiconductor B being sandwiched between two 10 Å thick layers of another fictitious semiconductor A, which are further sandwiched by thick layers of heavily doped semiconductor B. The work-function potential of semiconductor A exceeds that of B by 1.5 eV. The double-barrier structure with the applied field is shown in figure 3(*a*). Assuming that the effective masses of the barrier and the well regions are the same, which are $0.067m_0$, we get the transmission probability shown with the dashed curve in figure 3(*b*). To examine the importance of including the variation of the effective mass into the calculations, different effective masses in the semiconductors A and B are considered, which are $0.15m_0$ for semiconductor A and $0.067m_0$ for B. The transmission probability is shown with the solid curve in the same plot. The transmission probabilities for the two cases are compared in figure 3(*b*). The profiles of the two curves are similar to each other, however the maximum of the left peak is increased and the position of the left peak moves toward lower energy when the variation of the effective mass is included. The difference in the transmission probabilities for the two cases is obviously seen. The inclusion of the variation of the effective mass reflects more truth of the tunnelling, and we come to the conclusion that the influence of the effective mass should not be omitted. Comparing figure 3 with figure 2, we also see that

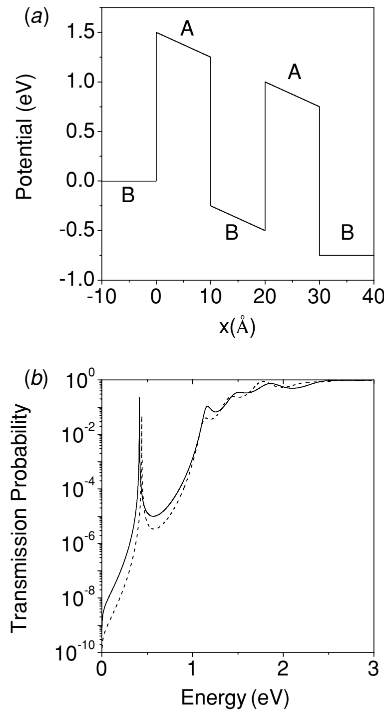


**Figure 3.** (*a*) The potential barrier of the superlattice structure consisting of layers of semiconductors A and B. (*b*) Transmission probability as a function of the incident electron energy for the structure in (*a*).

the asymmetry of both barriers affects the calculated transmission probability greatly. The breaking of the symmetry of the two barriers gives rise to a weakening of the resonances. The presence of asymmetric potentials leads to a reduction of the heights of the transmission peaks at resonance energies.

As shown above, our method is accurate in calculating the transmission probabilities in double-barrier structures with linearly varying potentials. To demonstrate the capability of our method for the double-barrier structure with non-linear potential, we further consider the double-barrier structure with a parabolic well, which is shown in figure 4(*a*). The double-barrier structure is fabricated with GaAs–$Al_aGa_{1-a}As$ ($a$:1–0–1). The parameter for the band offset is the same as that in the first example. For this system, assuming the variation of the composition $a$ is linear with the position $x$, we get

$$a(x) = \begin{cases} -(x+50)/50+1 & (-50 \leqslant x \leqslant 0) \\ (x-50)/50+1 & (0 < x \leqslant 50). \end{cases} \tag{26}$$

The effective mass $m(a)$ for the system satisfies the following equation

$$m(a) = (0.067 + 0.083a)m_0, \tag{27}$$

where $m_0$ is the free-electron mass. Then the position-dependent effective mass can be described by

$$m(x) = \begin{cases} (-0.083 \times (x/50) + 0.067)m_0 & (-50 \leqslant x < 0) \\ (0.083 \times (x/50) + 0.067)m_0 & (0 \leqslant x \leqslant 50) \\ 0.067m_0 & (x < -50, x > 50). \end{cases} \tag{28}$$

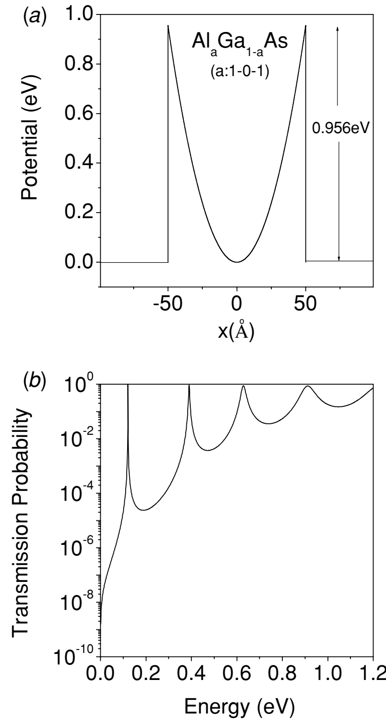


**Figure 4.** (*a*) Double barrier with a parabolic well made of GaAs and $Al_aGa_{1-a}As$. (*b*) Transmission probability as a function of the incident electron energy for the structure in (*a*).

The maximum potential energy is 0.956 eV for the double-barrier structure, as shown in figure 4(*a*). For the GaAs–$Al_aGa_{1-a}As$ ($a : 1 - 0 - 1$) system, the potential energy as a function of the position $x$ is as follows:

$$V(x) = \begin{cases} 0.956(x/50)^2 & (-50 < x < 50) \\ 0 & (x \leqslant -50, x \geqslant 50). \end{cases} \tag{29}$$

The unit of the position $x$ is Å.

In the double-barrier structure, the tunnelling resonance is found. As shown in figure 4(*b*), the peaks of the transmission probability separate at regular intervals for a parabolic well. We encountered in some of our calculations at very low values of incident energy numerical instabilities around the resonance energies, which can possibly be removed by employing the appropriate manipulation at energies close to the lower resonances. We divide the region near the lower resonances into more layers, so that the resonant peaks at low values of incident energy are not lost. In our practical manipulation the barrier is divided into $10^3$ layers for the incident electron energy varying from 0 eV to 0.01 eV, $10^3$ layers for the energy from 0.01eV to 0.1 eV and also $10^3$ layers for that from 0.1 eV to 0.2 eV, which is done step by step. The energy resonant peaks in a double-barrier system can be accurately obtained by the proposed method.

Another attractive feature of the analytical transfer matrix method is its ability to evaluate the eigenenergy of any potential well, which has been discussed in our previous results [15]. In the double-barrier structure with a parabolic well, the transmission probability reaches its absolute maximum of unity at $E_1 = 0.121$ eV, $E_2 = 0.390$ eV, $E_3 = 0.629$ eV and

$E_4 = 0.912$ eV, as shown in figure 4(*b*). The energy levels for the bound states of the included potential well from our analytical transfer matrix method are $E_1 = 0.1211$ eV, $E_2 = 0.3906$ eV, $E_3 = 0.6289$ eV and $E_4 = 0.9125$ eV. A comparison with the discrete levels of the included potential well shows that these peak energies occur near the bound state energies. Note that the transmission peak at the low energy ($E_1$) is considerably sharper than that at high energy ($E_2$) in figure 4(*b*), indicating that the associated bound states are more tightly bound. These results exhibit the striking effects of resonant tunnelling.

## 4. Conclusion

In conclusion, an alternative method for accurately calculating the transmission probability across an arbitrary potential barrier with dependence on the space of the effective mass is presented. This method differs from previous derivations in that mass variations from layer to layer are explicitly taken into account. Furthermore, we give the analytical formula describing the tunnelling properties on the basis of the analytical transfer matrix method. Mass variations are directly included in the analytical formula. Single-barrier and various double-barrier structures are analysed to confirm the validity and usefulness of the proposed method. Agreement is reached among the results obtained by our method and other methods. Various potential barriers, including continuous variations of potential and effective mass, can be analysed easily by using the present method. The method is universal and exact. With our analytical transfer matrix method, we can correlate the energy location of the peaks of the transmission probability with the bound state energies of the included potential wells. The present technique is expected to be exploited for analysing and designing resonant tunnelling and other quantum size effect devices.

## Acknowledgments

This work is supported by National Natural Science Foundation of China under grant no 60237010.

## References

[1] Koga T, Nitta J and Takayanagi H 2002 *Phys. Rev. Lett.* **88** 126601
[2] Chandra A and Eastman L F 1982 *J. Appl. Phys.* **53** 9165
[3] Schmitt L M 1999 *Appl. Phys.* A **68** 553
[4] Liu H C 1987 *Appl. Phys. Lett.* **51** 1019
[5] Ricco B and Azbel M Y 1984 *Phys. Rev.* B **29** 1970
[6] Yuk D, Ko K and Inkson J C 1988 *Phys. Rev.* B **38** 9945
[7] Vassell M O, Lee J and Lockwood H F 1983 *J. Appl. Phys.* **54** 5206
[8] Nakamura K *et al* 1991 *IEEE J. Quantum Electron.* **27** 1189
[9] Ando Y and Itoh T 1987 *J. Appl. Phys.* **61** 1497
[10] Allen S S and Richardson S L 1994 *Phys. Rev.* **50** 11693
[11] Jonsson B and Eng S T 1990 *IEEE J. Quantum Electron.* **26** 2025
[12] Sanada H 1997 *IEEE J. Quantum Electron.* **33** 731
[13] Vatannia S and Gildenblat G 1996 *IEEE J. Quantum Electron.* **32** 1093
[14] Lui W W and Fukuma M 1986 *J. Appl. Phys.* **60** 1555
[15] Cao Z *et al* 2001 *Phys. Rev.* A **63** 054103
[16] Miller R C, Kleinman D A and Gossard A C 1984 *Phys. Rev.* B **29** 7085